PHYSICAL REVIEW B VOLUME 2, NUMBER 8 15 OCTOBER 1970

X-Ray Diffraction Measurements on Metallic and Semiconducting Hexagonal NiS†

Jeffrey Trahan and R. G. Goodrich
Department of Physics and Astronomy, Louisiana State University, Baton Rouge, Louisiana 70803
and
S. F. Watkins
Coates Chemical Laboratory, Louisiana State University, Baton Rouge, Louisiana 70803
(Received 2 June 1970)

The crystallographic structure of hexagonal NiS has been determined at temperatures above and below the metal-semiconducting transition. The powder x-ray diffraction peak intensities were used to determine the atom positions in both phases. The symmetry of the unit cell is found to change from $P6_3/mmc(D_{6h}^4)$ in the metallic phase to $P6_3mc(C_{6v}^4)$ in the semiconducting phase.

I. INTRODUCTION

Of all of the compounds which are known to undergo a metal-to-insulator or metal-to-semiconductor (MS) transition as a function of temperature, only hexagonal NiS is magnetically ordered at exactly the same temperature as the MS transition.[1] This situation has made hexagonal NiS interesting theoretically since the magnetic ordering was the only experimentally observed mechanism which might be used to explain the semiconducting behavior below the Néel temperature. Prior to the present investigation, there had been no detailed determinations of the crystalline structure in the semiconducting phase of NiS, and it has been assumed that no structural change occurred at the transition.

Stoichiometric NiS crystallizes in two structures, a rhombohedral phase (millerite)[2] and a hexagonal phase (NiAs).[3] Although the rhombohedral phase is the stable phase at room temperature, the hexagonal phase can be made to exist stably at room temperature by quenching it from above 652 °K. This hexagonal phase exhibits a sharp MS transition at 265 °K.[4] In addition, neutron diffraction studies have shown that the material becomes antiferromagnetically ordered at this same temperature.[5] Below the transition temperature, the magnetic structure is found to be a simple two sublattice structure in which the magnetic moments of the Ni atoms are coupled ferromagnetically within {001} planes and antiferromagnetically between adjacent {001} planes. This results in the magnetic unit cell being identical to the chemical unit cell. Furthermore, it is found that the sublattice magnetization is within 10% of saturation upon ordering. There is apparently little or no magnetic moment associated with the Ni atoms above the transition in the metallic state.

In addition to the powder neutron diffraction studies of Sparks and Komoto,[4,5] measurements of the magnetic susceptibility and electrical resistivity through the transition have been made by the same authors.[6,7] These measurements along with the neutron diffraction data indicate that the transition is of first order, exhibiting considerable hysteresis and a volume change. The c/a ratio is observed to increase on cooling through the transition with the a and c lattice parameters increasing by 0.3 and 1%, respectively.[7] There is no indication from their data, however, of a change in lattice symmetry at the transition.

In the following sections the techniques of the present x-ray diffraction measurements are described along with the specific analysis to which they were subjected. From these measurements. it is concluded that a subtle change in the symmetry of the hexagonal structure does occur at the MS transition.

II. EXPERIMENT

The samples used in this experiment were prepared from high-purity Ni and S powders purchased from Johnson, Matthey and Company, Limited and American Smelting and Refining Company, respectively. The quoted impurity content in each case is less than 10 ppm. After reducing the Ni powder for several hours in a hydrogen atmosphere, equal atomic percentages of both were weighed and placed in a quartz tube which was then evacuated to the vapor pressure of S at 300 °K and sealed. These sealed tubes were then placed in an oven and the mixture was reacted at 400 °C. After the chemical reaction was complete, the NiS was raised above its melting point (~ 980 °C) for 1 h; the temperature was then lowered to 900 °C and left for 96 h. This high-temperature anneal homogenized the ingot, giving a uniform distribution of Ni and S throughout the rod. After annealing, the temperature was

slowly reduced to room temperature and the ingot removed from the quartz tube.

Powders for the x-ray measurements were made by grinding pieces from the ingot in a mixer mill and sieving them through a 400 mesh screen. This ensured that the particle size was less than 37 μ. The resulting powder was resealed in an evacuated quartz tube and annealed for 5 h at 500 °C and 6 h at 450 °C. It was found that annealing the powder at higher temperatures produced larger crystallites. After annealing, the powder was quenched to room temperature. This procedure resulted in single phase samples of uniform homogeneity. The composition was checked by chemical analysis and found to be (50.0 ± 0.02)% at Ni. These results are confirmed by the measured MS transition temperature which is a strong function of composition.[7]

The x-ray intensity data were taken with Ni-filtered Cu$K\alpha$ radiation on a General Electric diffractometer at both 300 and 77 °K. A check for preferred orientation in the samples on which the intensity data were taken was made by taking an x-ray transmission photograph of the prepared powder samples. This resulted in uniform ring intensities on the photographs, indicating that the powders were randomly distributed in orientation on the sample holder. In the intensity measurements, the peak widths (full width at half-maximum) varied from 0.25° at 30° to 0.45° at 150° (angles are given in 2θ). It is noted, however, that at low 2θ the $K\alpha_1$ and $K\alpha_2$ peaks were not resolved, whereas, they were at the higher angles. Some of the diffraction peaks were also observed through the MS transition which occurred between 266 and 267 °K. During these measurements, the temperature was stabilized with a heater and thermocouple arrangement, and the sample was left at each temperature (± 0.1 °K) for approximately 30 min to allow equilibrium to be reached.

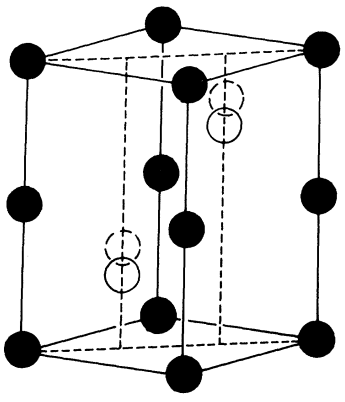

FIG. 1. Unit cell for the NiAs structure. The open circles represent the positions of the anions when the symmetry is $P6_3/mmc$ and the dashed circles their position when the symmetry is $P6_3mc$.

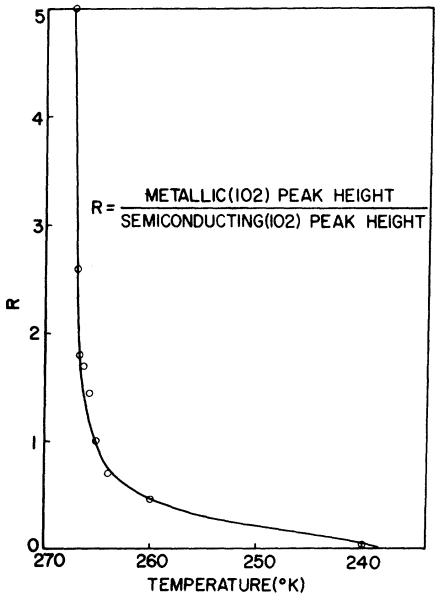

FIG. 2. Ratio of the (102) x-ray diffraction peak heights for the metallic and semiconducting phases of NiS as a function of temperature.

III. RESULTS AND DISCUSSION

The NiAs structure is shown in Fig. 1. In this structure, the large nonmetal anions form a hcp lattice, while the smaller metal cations compose a simple hexagonal lattice by occupying the octahedral interstitial sites of the hcp lattice. The tetrahedral sites are vacant. In the unit cell, the cations are at (0, 0, 0) and (0, 0, $\frac{1}{2}$) while the anions are located at ($\frac{1}{3}$, $\frac{2}{3}$, z) and ($\frac{2}{3}$, $\frac{3}{4}$, $z+\frac{1}{2}$).

When the temperature of NiS was slowly lowered, several new peaks appeared in the diffraction pattern at the MS transition temperature due to the appearance of the semiconductor phase. The angular separation of the low-temperature and high-temperature peaks was generally within 1 °2θ. As the temperature decreased, the low-temperature peaks gained in intensity at the expense of the high-temperature peaks, and a plot of the intensity ratio for the 102 reflection (Fig. 2) shows that the phase change is essentially complete within 7 °K of the MS transition temperature. No trace of the high-temperature phase was detected at 77 °K. Apparently both structures exist simultaneously just below the transition because of small local deviations in the composition of the sample. Tables I and II give the observed intensities and the observed and calculated structure factors for the sample at 300 and 77 °K.

Lattice parameters at the two temperatures were

TABLE I. Intensities and structure factors for hexagonal NiS at 300 °K.

h	k	l	Intensity (Counts)	Standard deviation	Observed structure factor	Calculated structure factor
0	1	0	4189	54	31.35	31.98
0	0	2	276	23	15.66	16.13
1	0	1	2697	46	20.67	19.22
1	0	2	5994	64	42.02	43.02
1	1	0	3199	50	51.82	50.35
1	0	3	363	28	14.25	15.18
0	2	0	301	28	18.97	19.96
1	1	2	133	25	9.24	8.33
0	2	1	323	30	14.55	14.55
0	0	4	319	32	38.41	35.17
2	0	2	1132	40	30.54	30.57
0	1	4	163	32	12.40	7.43
2	0	3	93	32	9.97	14.02
2	1	0	101	34	10.45	11.84
2	1	1	200	42	10.54	13.53
1	1	4	861	45	31.51	28.68
1	2	2	998	48	24.07	23.47
0	1	5	88	35	10.12	14.02
0	3	0	390	41	30.08	30.76
2	1	3	160	41	9.45	13.06
0	2	5	104	29	9.52	13.06
2	2	0	453	34	27.42	25.62
1	0	6	323	35	16.11	13.09
1	3	1	246	36	8.47	11.74
3	0	4	956	57	20.45	21.00

calculated by a least-squares procedure from the complete sets of diffraction maxima and are given in Table III. These results are in good agreement with those of Laffitte,[3] but the length of the c axis observed by us differs slightly from that measured by Sparks and Komoto.[4]

The reduced intensity data were used to compute Patterson (vector) maps at both temperatures with resolutions of 0.1 Å. The resulting maxima corresponding to Ni-S vectors were found to be spherical at 300 °K, but slightly elongated in the direction of the c axis at 77 °K. Significantly, neither the Ni-Ni nor the S-S vector maxima were distorted from sphereical symmetry at either temperature. These results are indicative of a shift of sulfur atoms with respect to the nickel atoms below the transition temperature.

The NiAs structure type is consistent with two possible space groups. The centrosymmetric model, space group $P6_3/mmc$ (D^4_{6h}, number 194),[8] restricts the nickel atoms to $2a$ positions and the sulfur atoms to $2c$ positions ($z = 0.250$). In the noncentrosymmetric model, space group $P6_3mc$ (C^4_{6v}, number 186),[9] the Ni atoms are again restricted to the origin, (0, 0, 0), but the S atoms in $2b$ positions may assume effectively any value of z.

In all four refinement models, the function minimized was $\sum w(\Delta F)^2$, where the sum is taken over all observed diffraction maxima, w is the weight of each observation derived from counting statistics, and ΔF is the difference between the observed and calculated structure factors. Each calculated structure factor is modulated by a temperature factor $\exp(-\frac{1}{4}\vec{s}\cdot\mathbf{B}\cdot\vec{s})$, where $\vec{s}$ is the reciprocal lattice vector of length $2\sin\theta$ and $\mathbf{B}$ is the anisotropic thermal displacement tensor. Only the B_{11} and B_{33} components are independent since the remaining four elements of this symmetric tensor are related by space-group symmetry as follows: $B_{11} = B_{22} = 2B_{12}$, $B_{13} = B_{23} = 0$.

The crystallographically independent unit in each space group effectively contains only one Ni and one S. Thus, five parameters, including two thermal parameters for Ni and two for S as well as a data scaling factor, were adjusted in the centrosymmetric models. The atomic scattering factors used were those of Ibers.[8] The final weighted residual factors $\{R = [\sum w(\Delta F)^2/\sum w|F_0|^2]^{1/2}\}$ for all four refinement models are shown in Table IV.

At 300 °K, the R value for the constrained and unconstrained models are identical. In addition, the position of S differs from 0.250 in the noncen-

TABLE II. Intensities and structure factors for hexagonal NiS at 77 °K.

h	k	l	Intensity (Counts)	Standard deviation	Observed structure factor	Calculated structure factor
0	1	0	4320	50	31.57	32.28
0	0	2	392	21	18.38	19.68
1	0	1	2818	41	20.90	19.47
1	0	2	6531	61	43.25	44.15
1	1	0	3571	63	54.28	51.96
1	0	3	369	23	14.14	15.35
0	2	0	348	24	20.24	20.74
1	1	2	152	22	9.78	11.56
0	2	1	323	23	14.42	15.21
0	0	4	286	27	41.60	35.58
2	0	2	1418	46	33.83	32.25
0	1	4	272	28	15.78	12.24
2	0	3	149	28	12.43	14.65
2	1	0	155	27	12.83	12.64
2	1	1	260	28	11.93	14.62
1	1	4	890	47	31.76	29.67
1	2	2	1132	38	25.46	25.46
0	1	5	147	35	13.00	14.17
0	3	0	488	36	33.42	33.82
0	2	4	104	30	10.95	8.20
2	1	3	192	32	10.30	14.12
0	2	5	86	44	8.74	13.65
2	1	4	172	34	8.53	5.94
2	2	0	522	65	29.39	29.10
1	3	1	315	54	9.61	13.56
3	0	4	1157	77	23.14	22.95

TABLE III. Lattice parameters, temperature coefficients, and positions of S atoms at 300 and 77 °K. Standard deviations are shown in parentheses.

Temperature (°K)	Lattice Parameters (Å)		Components of thermal displacement tensor				Position of S atoms
	a	c	B_{11}(Ni)	B_{33}(Ni)	B_{11}(S)	B_{33}(S)	z
300	3.4395(2)	5.3514(7)	0.054(16)	0.038(5)	−0.004(13)	−0.004(5)	0.250
77	3.4456(8)	5.405(1)	0.044(15)	0.031(6)	−0.015(15)	−0.004(7)	0.275(7)

trosymmetric model by less than one estimated standard deviation. It must therefore be concluded that the crystal structure of NiS in the metallic state is centrosymmetric. However, at 77 °K, the R value decreases when the centrosymmetric constraint on the sulfur position is released. The R factor ratio test of Hamilton[10] indicates that this decrease is significant at the 90% confidence level. Further, z varies significantly (more than 3σ) from 0.250, and the estimated standard deviation is small and reasonable. These results, together with the evidence from the Patterson syntheses, lead us to conclude that NiS in the semiconducting state is noncentrosymmetric.

The values of the thermal displacement tensor components shown in Table III are not physically meaningful since the sulfur tensors are marginally nonpositive definite and correspond to negative rms displacements. Nevertheless, our conclusions concerning the atomic positions and the change in crystal structure are not mitigated by these results. Rather, these results indicate that a slight disordering of the nickel and sulfur atoms may exist in this sample at both high and low temperatures, although the extent of interchange cannot be established.

Further support for a slightly disordered structure, and evidence of the over-all correctness of these two crystal structures, is furnished by the weighted electron density difference synthesis. Neither the centrosymmetric high-temperature structure nor the noncentrosymmetric low-temperature structure displayed residual electron density peaks above 0.7 electrons Å^{-3} except at the tetrahedral interstitial sites. At these positions, prominent residual peaks of 1.8 electrons Å^{-3}, corresponding to approximately 0.09% Ni, were observed. These observations support the conclusion of Sparks and Komoto[7] that no abrupt change in the disorder occurs over the transition.

TABLE IV. R values for structure refinements for different temperatures and symmetries.

Temp (°K)	Space group	Number of parameters refined	z	R
300	$P6_3/mmc$	5	0.25 (constrained)	0.047
300	$P6_3mc$	6	0.237 ± 0.016	0.047
77	$P6_3/mmc$	5	0.25 (constrained)	0.052
77	$P6_3mc$	6	0.275 ± 0.007	0.049

The change in the NiS crystal structure which occurs over the MS transition is subtle but significant. Above 266 °K, both the S and Ni atoms are in nearest-neighbor environments of octahedral symmetry. At the transition temperature, a concerted S atom shift of 0.134 Å toward the hexagonal nickel basal planes places the S and Ni atoms in local crystal fields of C_{3v} symmetry. The six Ni-S distances change from 2.394 Å at 300 °K to 2.483 and 2.331 Å at 77 °K, while the unit-cell volume shows a 1.3% increase on lowering the temperature from 300 to 77 °K. This change in symmetry will lift some of the degeneracies existing in the band structure of the metallic phase and gives a second possible mechanism for the MS transition.

In view of this structural change, it is not surprising that NiS single crystals fracture upon cooling, an observation first noted by Sparks and Komoto[6] and confirmed by Laue photographs on our samples. We conclude that further single-crystal studies on the low-temperature phase would be virtually impossible. This report is the first in a series of a systematic experimental study of the MS transition in hexagonal NiS currently in progress in this laboratory.

†Work performed under the auspices of the U.S. Atomic Energy Commission, A. E. C. Report No. ORO-3087-40.

[1]For a review of most of the existing theories for the metal-insulator transition in transition-metal compounds see David Adler, Rev. Mod. Phys. 40, 714 (1968).

[2]N. H. Kolkmeijer and A. L. Th. Moesveld, Z. Krist. 80, 91 (1931).

[3]M. Laffitte, Bull. Soc. Chim. France 1959, 1211 (1959).

[4]J. T. Sparks and T. Komoto, J. Appl. Phys. 34, 1191 (1963).

[5]J. T. Sparks and T. Komoto, J. Appl. Phys. 39, 715 (1968).

[6]J. T. Sparks and T. Komoto, Phys. Letters 25A, 398 (1967).

[7]J. T. Sparks and T. Komoto, Rev. Mod. Phys. 40, 752 (1968).

[8]*International Tables for X-Ray Crystallography* (Kynoch Press, Birmingham, England, 1965), Vol. III, p. 201.

[9]See Ref. 8, Vol. 1.

[10]Walter C. Hamilton, Acta Cryst. 18, 502 (1965).

PHYSICAL REVIEW B VOLUME 2, NUMBER 8 15 OCTOBER 1970

Long-Range Forces between Molecules and Metals

D. Lando* and L. J. Slutsky
Department of Chemistry, University of Washington, Seattle, Washington 98105
(Received 17 April 1970)

Isotherms of oxygen, argon, neopentane, tetramethylsilane, and diethyl ether on optically flat gold surfaces have been determined over the range 0–70 Brunauer-Emmett-Teller (BET) monolayers, corresponding to 0–220 Å. The results are found to imply a potential energy of interaction $U(Z)$ of the form $U(Z) = \alpha 1.74\times10^{-4}Z^{-2}$ erg/molecule, where α is the molecular polarizability and Z the distance from the surface. The possible source of the disagreement between the experimental results and the theoretical predictions of Margenau, Bardeen, and Lennard-Jones is briefly discussed.

INTRODUCTION

The potential energy $U(Z)$ of a molecule at distance Z from a conducting surface has been the object of extensive theoretical investigation. Lennard-Jones,[1] Margenau and Pollard,[2] and Bardeen[3] evaluate the energy of the interaction of the instantaneous dipole moment of the molecule with its image in the metal and so deduce a potential proportional to Z^{-3}. Mavroyannis[4] and Dzyaloshinskii *et al.*[5] obtain this result at distances where retardation is not important; a potential which varies as Z^{-4} is predicted at greater distances.[4–7] Prosen and Sachs[8] calculate the energy of an assembly of free electrons and ion cores in the field of an external molecule by means of second-order perturbation theory and arrive at a potential of the form $Z^{-2}\ln 2k_FZ$, where k_F is the magnitude of the Fermi wave vector.

The limiting form of the Frenkel-Halsey-Hill equation[9–10] provides a connection between $U(Z)$ and experimentally accessible quantities. The equilibrium vapor pressure of an adsorbed film of thickness Z is given by

$$\ln(P/P^0) = -[U(Z) - U'(Z)]/kT = -\Delta U(Z)/kT, \quad (1)$$

where P^0 is the equilibrium vapor pressure of the bulk adsorbate and $U'(Z)$ the potential energy of a molecule at distance Z from a semi-infinite slab of bulk adsorbate. We have investigated the adsorption of methanol and diethyl ether on optically flat gold surfaces at coverages between 0 and 70 BET monolayers (corresponding to film thickness 0–220 Å). As found previously for the pseudospherical molecules neopentane and tetramethylsilane,[11] the limiting form of the potential at large values of Z is $U(Z) = \alpha CZ^{-2}$, where α is the molecular polarizability.

EXPERIMENTAL

The deposition of a small mass (Δm) on the surface of a quartz crystal of total mass m vibrating in a thickness shear mode produces a change (Δf) in the resonant frequency (f) given by

$$\Delta f/f = \Delta m/m\ . \quad (2)$$

Since Δf can be measured with considerable accuracy, such a crystal constitutes a rather sensitive adsorption microbalance.[12,13] When the adsorbed film is sufficiently thick so that its density may be approximated by the density (ρ) of the bulk adsorbate, Eq. (2) may be rewritten in terms of the film thickness Z as $Z = (\rho_q t_q/2K\rho f)\Delta f$, where ρ_q is the density of quartz, t_q is the thickness of the quartz crystal, and the "roughness factor" K is the ratio of the "true surface area" of the crystal to the geometrical area. The form of $\Delta U(Z)$ can thus be deduced directly from the very high coverage portion of the adsorption isotherm, the numerical evaluation of $\Delta U(Z)$ requires an independent determination of K.

There is experimental evidence in support of an inverse-cube law for the potential between molecules and nonmetals and reason to believe[14,15] that the Kirkwood-Muller formula[16] gives a qualitatively correct account of the magnitude of the interaction. We have attempted here to evaluate $\Delta U(Z)$ in the region where $U'(Z)$ is expected to be negligible and so characterize $U(Z)$ independently of an exact form for $U'(Z)$.

The apparatus used in this work is illustrated schematically in Fig. 1. A 5-MHz AT-cut quartz